

**LIBS PLASMA DIAGNOSTICS WITH SUPERCAM ON MARS.** H.T. Manelski<sup>1</sup>, R.C. Wiens<sup>1</sup>, S. Schröder<sup>2</sup>, P.B. Hansen<sup>2</sup>, B. Bousquet<sup>3</sup>, N. Martin<sup>4</sup>, and S. Clegg<sup>4</sup>, <sup>1</sup>Purdue University, Lafayette, IN, USA, <sup>2</sup>Deutsches Zentrum für Luft- und Raumfahrt (DLR), Institut für Optische Sensorsysteme, Berlin, Germany, <sup>3</sup>Centre Laser Intenses et Applications, CNRS, Université de Bordeaux, Bordeaux, France, <sup>4</sup>Los Alamos National Laboratory, Los Alamos, NM, USA

**Introduction:** The SuperCam instrument on the Perseverance rover utilizes a variety of techniques to constrain the chemistry and mineralogy of geologic materials that the rover encounters on Mars [1,2]. Laser Induced Breakdown Spectroscopy (LIBS) is a versatile method used by SuperCam for rapid and in-situ quantification of major elements in geologic materials. LIBS is particularly valuable because of its ability to clear the ubiquitous Martian dust and effectiveness over a range of distances [1,2]. In LIBS, a laser is fired at a target and a plasma is generated. As the electrons in the plasma decay back to lower energy states, photons are emitted with energies specific to the various elements present in the sample. The observed emission lines are strongly influenced by the physical conditions in the plasma plume. Specifically, plasma temperature and electron density can affect the strength and visibility of spectral lines [3]. In this work, we present estimates for plasma temperatures and electron densities of laser-induced plasmas on Mars with the SuperCam instrument on the Perseverance rover which indicate relatively stable plasma dynamics across a range of sample types and distances.

**Methods:** When a plasma is in thermodynamic equilibrium, the electrons, atoms, and ions present can be fully described by statistical mechanics, where the equilibrium distribution is defined by the temperature [4]. When the condition of Local Thermodynamic Equilibrium (LTE) can be assumed, this plasma temperature can be estimated based on the relative strengths of spectral lines. Specifically, the intensity of spectral lines can be described by a Boltzmann distribution and can be related to various atomic parameters via the equation below [4]:

$$\ln(I\lambda/gA) = -E_U/kT - \ln(4\pi Z/hcN_0),$$

where  $I$  is the spectral line radiant intensity,  $\lambda$  is the wavelength of the transition,  $g$  is the degeneracy,  $A$  is the transition probability,  $E_U$  is the upper energy of the emission,  $k$  is the Boltzmann constant,  $T$  is the temperature,  $Z$  is the partition function,  $h$  is Planck's constant,  $c$  is the speed of light, and  $N_0$  is the total species population.

Plotting  $\ln(I\lambda/gA)$  against the upper energy level ( $E_U$ ) will therefore result in a straight line with a slope of  $-1/kT$ , if there is a Boltzmann distribution. It is by this method that plasma temperatures were estimated for Fe I, Ca I, and Ti II. Many spectral lines were examined; lines were chosen based on strength at a variety of

distances, upper energy spread, and lack of known interferences.

Integrated line intensities for nine Ca I, eleven Fe I, and sixteen Ti II lines were measured for all SuperCam LIBS spectra taken on Mars up to sol 961. Only lines within a given spectrometer (UV, VIO, and VNIR) were used for each species to minimize instrumental effects. Emission lines were fitted using a Lorentzian profile [5].

Electron densities were calculated based on the Stark broadening of the H- $\alpha$  line (656.467 nm). Stark broadening is the result of collisions between electrons and ions within the plasma. The relationship between Stark broadening and electron density has been theoretically and experimentally determined [6,7]:

$$\text{FWHM} = 1.098 \text{ nm} \times \left( \frac{N_e}{10^{23} \text{ m}^{-3}} \right)^{0.67965},$$

where  $N_e$  is the electron number density and FWHM is the full width at half maximum of the emission line. Instrumental peak widths were subtracted from the observed FWHM of the emission line to obtain the true Stark broadening.

LIBS plasmas on Mars do not capture LTE conditions because they are observed over a relative long time ( $>10 \mu\text{s}$ ) relative to plasma dynamics. To address this issue, time-resolved LIBS measurements were taken at Los Alamos with the SuperCam engineering qualification model (EQM) to examine the stability and temporal evolution of measured plasma temperatures and electron densities in Mars-like atmospheric conditions.

**Results:** Ca I and Fe I Boltzmann plots were generally well correlated, with most spectra having  $R^2 < -0.8$  (Fig. 1).

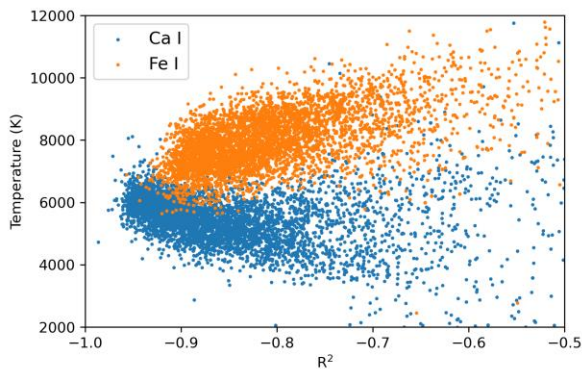


**Figure 1:** Plasma temperature (Ca I and Fe I) plotted against  $R^2$  (coefficient of determination) of the corresponding Boltzmann plot for SuperCam Mars LIBS spectra.

Boltzmann plots constructed using Ti II were poorly correlated. As the focus is on the most reliable temperature estimates, Ti II temperatures will be largely disregarded in this work. The most well correlated Ca I and Fe I Boltzmann plots indicate an average plasma temperature of 6000 to 8000 K (Fig. 1).

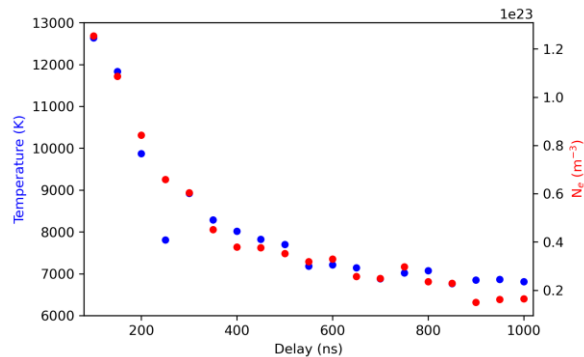


**Figure 2:** Ca I plasma temperature (left) and electron number density (right) vs time delay from a LIBS spectrum of a gypsum sample taken at LANL with SuperCam EQM. Taken with a time-gate of 100 ns moving in 50 ns intervals to 1 microsecond.

Ca I plasma temperatures and electron densities peak in the earliest observed time-gates at  $\sim 13000$  K and  $\sim 1.2 \times 10^{23} \text{ m}^{-3}$ , respectively (Fig. 2). It is worth noting that with SuperCam Mars data (averaged over  $\geq 10 \mu\text{s}$ ), neutral iron and calcium lines, whose emissions are longer lived, will have Boltzmann plots which reflect the more stable conditions of the plasma after  $\sim 400$  ns. Ionized species like Ti II will have more poorly correlated Boltzmann plots and higher apparent temperatures, reflecting the more transient early stage of plasma emission ( $< 400$  ns). The  $\geq 10 \mu\text{s}$  integration time likely explains the lower than expected LIBS plasma temperatures on Mars.

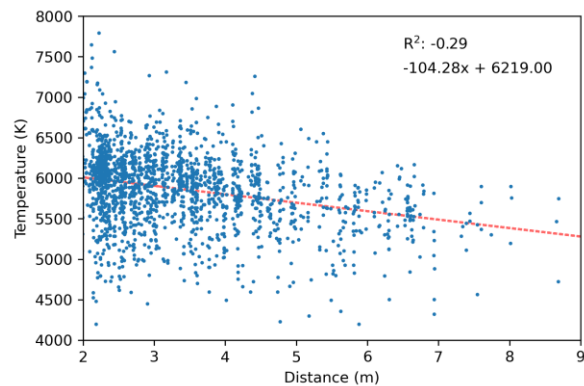


**Figure 3:** Ca I apparent plasma temperature vs distance for SuperCam Mars data. Only temperatures derived from Boltzmann plots with  $R^2 < -0.9$  are shown. Line of best fit shown in red.

There is a weak negative correlation between temperature and distance (Fig. 3) but this amounts to  $< 500$  K over SuperCam's typical LIBS range (2-6.5 m), indicating relatively stable plasma conditions.

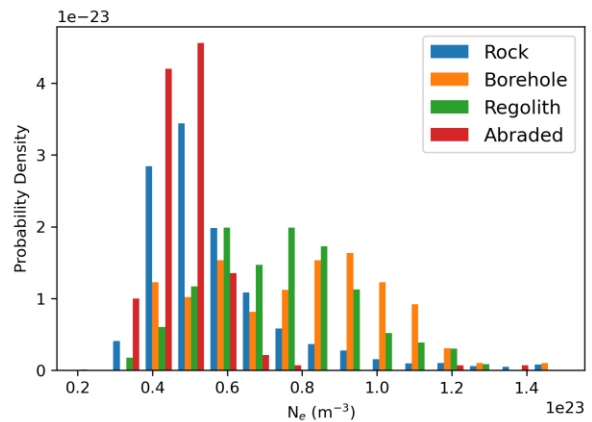


**Figure 4:** Probability density histogram of electron density for all SuperCam Mars LIBS spectra, colored by target type.

Electron densities derived from SuperCam Mars data demonstrate a clear relationship with target type. Rock targets and abraded patches have, on average,  $\sim 0.3 \times 10^{23} \text{ m}^{-3}$  lower electron density than regolith and borehole targets. This could be the result of increased plasma confinement on rough targets or more complex plasma-surface interactions, as explored in Rapin et al. 2017 [8] and Martin et al. [9].

**Discussion:** In this abstract, estimates for plasma temperature and electron density from SuperCam Mars LIBS spectra were presented. There is a weak negative correlation between plasma temperature and distance, but this amounts to  $< 500$  K within the range of distances of typical SuperCam LIBS observations on Mars. Electron densities were observed to vary significantly between target types (rocks vs regolith), highlighting the need to better understand the effect of plasma-surface interactions on LIBS emissions. We are continuing to explore any possible effects on SuperCam's calibration.

**References:** [1] Wiens R. C. et al. (2021) *Space Sci. Rev.*, 217, 4. [2] Maurice S. et al. (2021) *Space Sci. Rev.*, 217, 47. [3] Lepore K. H. et al. (2023) *GRL*, 50, 8. [4] Bousquet B. et al. (2023) *Spectrochimica Acta Part B: Atomic Spectroscopy*, 204. [5] Newville M. et al. (2014) *Zenodo*. [6] Gigosos M. A. et al. (2003) *Spectrochimica Acta Part B: Atomic Spectroscopy*, 58, 1489-1504. [7] Burger M. and Hermann J. (2016) *Spectrochimica Acta Part B: Atomic Spectroscopy*, 122, 118-126. [8] Rapin, W. et al. (2017) *Spectrochimica Acta Part B: Atomic Spectroscopy*, 137, 13-22. [9] Martin et al. this meeting